International Conference on Space Optics—ICSO 2022

Dubrovnik, Croatia

3–7 October 2022

Edited by Kyriaki Minoglou, Nikos Karafolas, and Bruno Cugny,

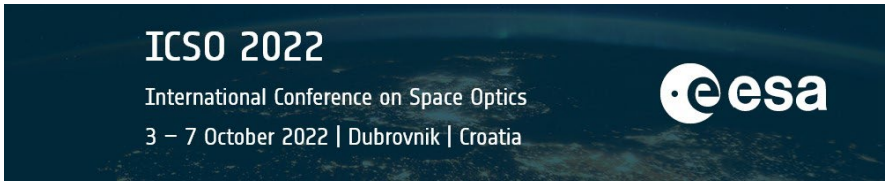

Report on a refractive static Fourier transform spectrometer flown on a stratospheric balloon for the HEMERA program

International Conference on Space Optics — ICSO 2022, edited by Kyriaki Minoglou, Nikos Karafolas, Bruno Cugny, Proc. of SPIE Vol. 12777, 127775G · © 2023 ESA and CNES · 0277-786X · doi: 10.1117/12.2691025

Report on a refractive static Fourier transform spectrometer flown on a stratospheric balloon for the HEMERA program

Lorenzo Cocola[a], Fabio Frassetto[a], Riccardo Claudi[b], Vania Da Deppo[a], Paola Zuppella[a], and Luca Poletto[a]

[a]CNR-IFN Padova, Via Trasea 7, 35131 Padova, Italy
[b]Astronomical Observatory, INAF, Padova, Italy

ABSTRACT

In this work, we report on the results obtained from a stratospheric balloon flight aimed to test a static Fourier transform spectrometer realized with Littrow prisms as retro- dispersive elements. Static Fourier Transform spectrometers are traditionally realized with reflecting diffractive gratings. In the flown optical configuration, the gratings were substituted with refractive-reflective prisms (Littrow prisms). The idea is that, besides the medium resolution obtainable with prisms, due to the dispersive power of the glasses, the optical quality of Littrow prisms can provide low noise instruments at low price. The reported results obtained with this technological demonstrator flight cover different aspects as the stability of the instrument and the signal to noise ratio. The flight took place in October 2021 at the CNES "Centre d' Opérations Ballons" at Aire sur l' Adour, France. The instrument acquired daylight (the flight started at about 10:00 AM) atmospheric spectra in the 600 – 800 nm spectral region with a spectral resolution of circa 700. The maximum reached altitude was about 28 km and the flight lasted about 2 hours. The payload had no pointing capabilities, and the on-board software was programmed to regulate the gain during the acquisitions due to the different conditions of illumination. Each acquisition consists of a 2D image, called interferogram, whose Fourier transform gives the spectral information of the entering light. The on-board computer is a Raspberry Pi; besides the interferograms, other data were acquired as temperature, pressure, payload orientation and position. This work has been supported by ASI, Agenzia Spaziale Italiana, Agreement n. 2019-33- HH.0, for the payload realization and the flight opportunity has been provided by the European Commission in the frame of the INFRAIA grant 730790-HEMERA.

Keywords: FTS, Spectroscopy, Stratospheric Balloon

1. INTRODUCTION

Static Fourier transform spectrometers (S-FTS) are nowadays well consolidated instruments. Compared to dispersive instruments, S-FTS can provide some peculiar features but, obviously, their suitability depends on the particular application. For a general introduction to the technique we propose to the reader some papers: 1, 2, 3, 4, 5 6 and 7. In this work we present the preliminary results obtained with a technical demonstrator in which the diffractive gratings are replaced with refractive-reflective prisms (Littrow prisms). The idea is that, for low resolution instruments, Littrow prisms can be a valuable substitute for the reflective gratings, providing less diffuse light and being economically advantageous.

2. THE INSTRUMENT

The optical concept of the instrument is schematized in Fig. 1 a). It is a traditional S-FTS with the gratings replaced by Littrow prisms. A detailed description of this variation to the classical optical concept can be found in 8, 9 and 10. Figure 1 b) is an image of the interferometric section, corresponding to the dashed area in 1 a). This base supports the beamsplitter and the two prisms. The tilt (α angle in 1 a)), bench plane alignment (β angle in 1 a)) and optical path length offset for each prism can be finely tuned using adjustment screws. A front

Further author information: (Send correspondence to L.C. and F.F.)
L.C.: E-mail: lorenzo.cocola@cnr.it, Telephone: +39 049 981 8262
F.F.: E-mail: fabio.frassetto@cnr.it, Telephone: +39 049 981 7447

mask is used to clamp the prisms and hold them in position. In order to minimize the possible deformation of the interferometric section, the connection elements between the interferometric base and the aluminium flight frame (***G*** in 1 b)) are realized as flexural elements and decoupled with elastic bushings.

The entire payload (corresponding to the interferometric base equipped with the entrance and exit optics, the onboard computer (OBC) and the battery pack) is shown in Fig 2. Figure 2 a) is an image of the whole payload, figure 2 b) is an image of the payload ready for the flight. The exterior of the payload has been realized with an expanded polystyrene (EPS) box, while the protruding entrance optics has been covered with an expanded polyethylene (EPE) hollow cylinder. All the opto-mechanical parts, OBC and batteries are connected to an aluminum frame. The energy necessary for the flight has been provided by eight AA-size lithium primary batteries.

The OBC, used for the acquisition of both the interferograms and the house keeping signals, is a *Raspberry pi 4 Model B*. Environmental parameters and payload attitude determination have been acquired via the use of dedicated modules: *BME 680* (temperature, pressure, gas and humidity), *BNO 055* (orientation and temperature) and *MTK3339* (positioning). The onboard software (OBS) has been designed so that every second all the house keeping signals and an interferogram were acquired.

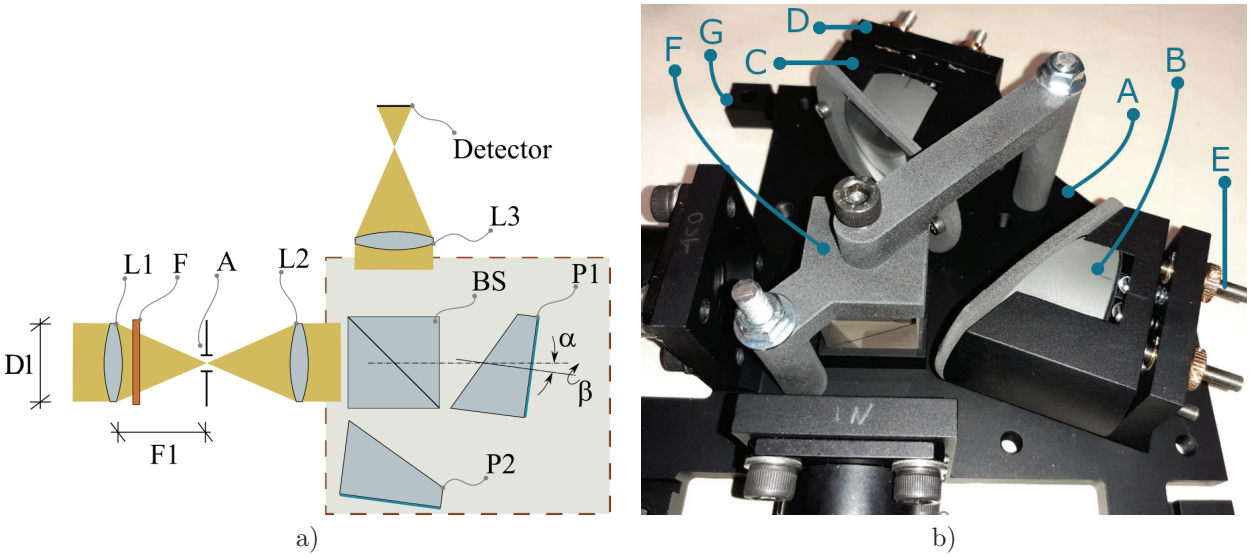

Figure 1. a) Schematic representation of the S-FTS: ***D1*** entrance aperture diaphragm, ***L1*** condenser lens, ***F1*** focal length of the condenser lens, ***F*** band-pass filter, ***A*** field aperture, ***L2*** collimating lens, ***P1,P2*** Littrow prisms and ***L3*** imaging lens. b) Image of the interferometric section: ***A*** interferometric base, ***B*** Littrow prism, ***C*** support of the Littrow prism, ***D*** adjusting base, ***E*** screws used to adjust the tilt of the prisms, ***F*** beam-splitter (under holding clamp) and ***G*** connecting point between the interferometric base and the aluminum frame.

The main opto-mechanical parameters of the spectrometer are summarized in table 1.

Before the flight the instrument has been tested for vacuum and thermal tests. A vacuum test of the electronic components, OBC and detector was performed at room temperature down to 10 mbar pressure. Another test, performed at ambient pressure, was conducted on the whole spectrometer assembly in a climatic chamber operating from -50 to +50 °C while acquiring light from a 633 nm He-Ne laser source. Those tests respectively proved the suitability of the chosen active components for an environment with almost only radiative cooling and the thermal stability of the optical bench, with an estimation of the total expected thermal drift.

3. THE FLIGHT

The flight took place at the CNES "Centre d'Opérations Ballons" at Aire-sur-l'Adour France (43.7001 N, 0.2623 W). The flight started at the 09:51 UTC of the 14-th of October 2021, the payload reached a maximum altitude

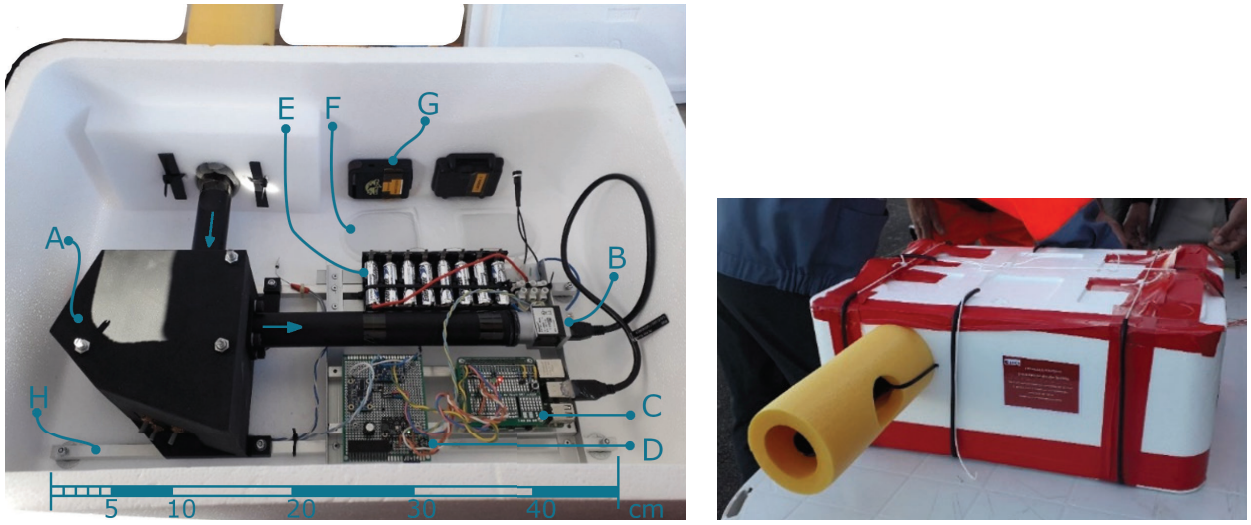

a) b)

Figure 2. a) Assembly of the payload, the scale on the bottom gives an indication of the total volume of the instrument. ***A*** interferometer, ***B*** detector, ***C*** Raspberry Pi 4 Model B, ***D*** additional electronic circuitry for power supply and environmental sensors, ***E*** batteries, ***F*** chemical heating pads, ***G*** tracking transponders (for recovery, provided by CNRS), ***H*** aluminum support frame. b) Payload arranged for the flight.

Table 1. Main parameters of the payload.

FOV	± 0.2 deg
F/#	f/9
A in Fig. 1 a)	1.5 mm diameter
D1 in Fig. 1 a)	23 mm diameter
F1 in Fig. 1 a)	200 mm
F in Fig. 1 a)	Interferential filter *Semrock 709/167*
BS in Fig. 1 a)	50/50 non polarizing
Total mass	2772 g
Total envelope	540 mm X 370 mm X 200 mm (20 mm thickness)
Resolution	680 @ 700 nm
$\Delta\lambda$ per pixel	0.55 nm (mean)
Detector	Basler acA 1920-40 um
Batteries	8 X AA-size, lithium, primary

of 27813 m at the 11:05 UTC and the flight terminated at the 12:00 UTC of the same day. The pressure and external temperature profile acquired during the ascending and descending phases are plotted in Fig. 3 a). The footprint of the entire flight is represented in Fig. 3 b), with the color representing the vertical altitude: the starting location (START), the point of maximum altitude (MAX HEIGHT) and the landing site coordinates (END) are identified with arrows.

4. DATA

During the flight an interferogram has been acquired every second. The integration time has been set to 50 ms in order to limit the effect of vibrations. The *auto-gain* function (available from the Basler library) has been

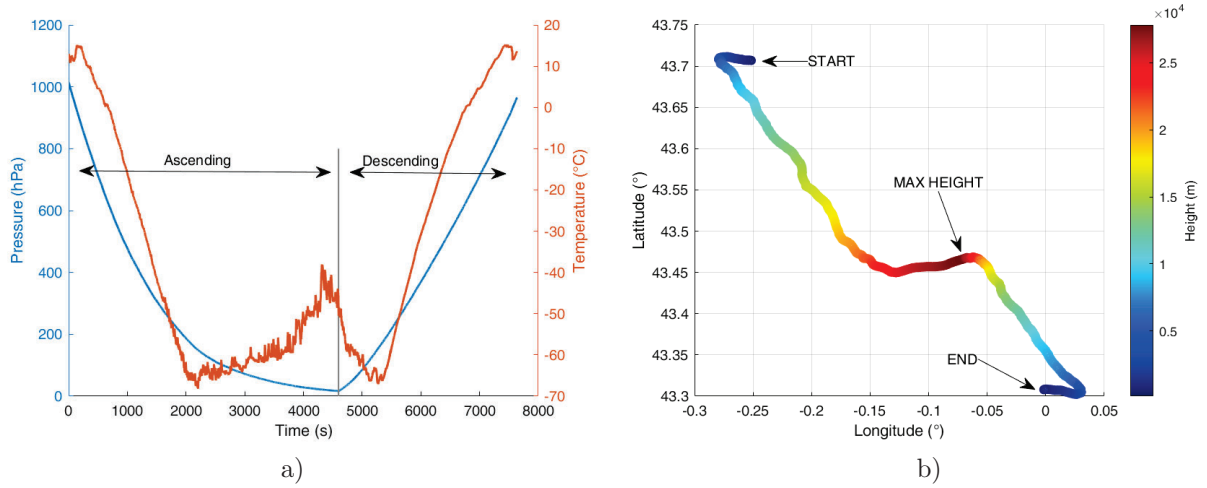

Figure 3. a) Pressure and external temperature as function of the time. b) Latitude and longitude of the payload during the flight. The colors represent the height in meters.

used to adjust the gain parameter during the acquisition, in order to deal with variable illumination conditions while limiting the number of saturated or dark images.

An example of some typical interferograms acquired during the flight is presented in Fig. 4. This figure is divided into five rows, each one refers to the signal acquired at a different altitude. The correspondence between the labels A-E and the corresponding altitude is presented in 5 a). The five points have been selected in order to cover the entire ascending phase, and in a way that provides an indication about instrumental effects due to thermal changes. The choice to limit the analysis only to the ascending phase is due to the fact that the descending one has been more turbulent, and the interferograms appear more unstable.

In each row of Fig. 4, on the right side is presented a detail of the acquired interferogram while on the left side is plotted the corresponding spectrum (obtained using the entire acquired interferogram). The part of the interferogram used to present the different interferogram details is the same for all the five points, as it is clear looking at the dust and speckle pattern in the image.

All the spectra are obtained multiplying the interferogram with a *Blackman* filter, applying the Fourier transform operator, calculating the square of the modulus and normalizing the result to the maximum in the interval 50-200 pixels (all the spectra have the maximum value normalized to one). The 621.2 nm and 794.4 nm are the two wavelengths corresponding to the 0.5 % transmission of the bandpass filter "F". Other two spectral features are indicated at 656.3 nm and 759.4 nm. The details of the interferograms show a change in the inclination of the interference fringes. This phenomenon has been also seen during the thermal tests, and is attributed to the thermal deformation of the interferometric base. The result of all the thermal deformations is an evident translation of the spectral content, visible looking at the pixel scale on each panel. A secondary, minor effect is a variation in the number of the pixels supporting the instrumental spectral band. This minor effect is evident by looking at the calibration curve in Fig. 5 b). All the spectra have been aligned to the 621.2 nm filter cut-in wavelength.

For each one of the five spectra in Fig. 4, a polynomial fit of the third order has been calculated; the number of the spectral features used for the fit differs in each one of the five cases depending on the number of reliably identifiable spectral references. For each fit, the residual errors are plotted in the bottom panel of Fig. 5 b). The maximum error is of the order of $\pm$ 1 nm. This uncertainty is mainly due to the difficulty of identifying spectral absorbance structures or in some cases the cutoff edge of the filter near 800 nm.

The spectra acquired during the flight are reported in Fig. 6. On Fig. 6 a) a stack of all the acquired spectra is shown. The conditions of pressure and temperature at which each spectrum has been acquired are plotted in the left side of the panel. Spectra originating from saturated frames or from frames with a non acceptable level

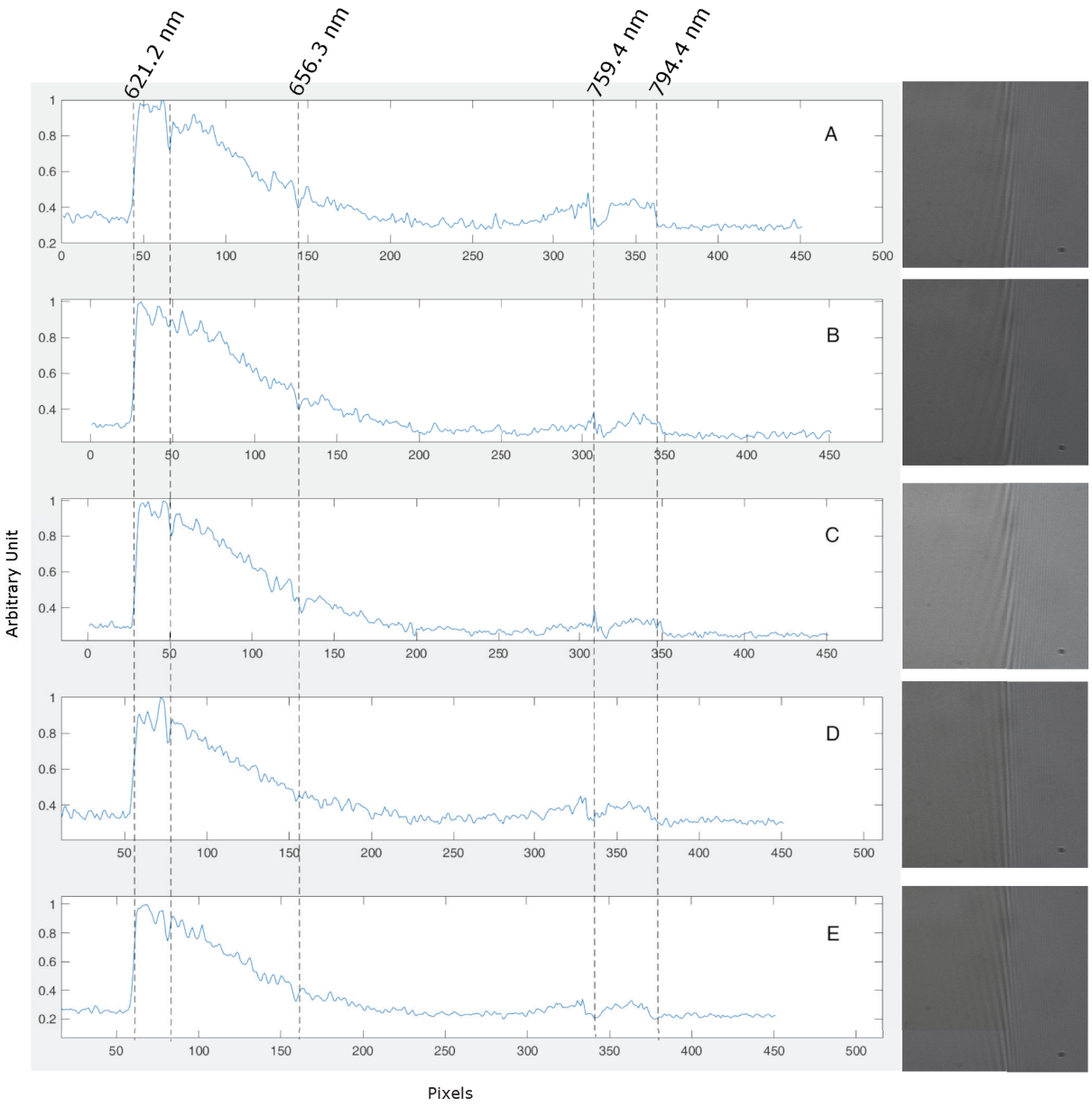

Figure 4. Mosaic of five spectra acquired during the ascending phase. On the right side of each panel, a detail of the corresponding interferogram is presented. The five letters A-E correspond to the five altitudes individuated with the same letters in Fig. 5 a).

of signal are removed (and appearing as dark rows). It is evident that at the time corresponding to the balloon explosion the acquisition manifests some stability problems.

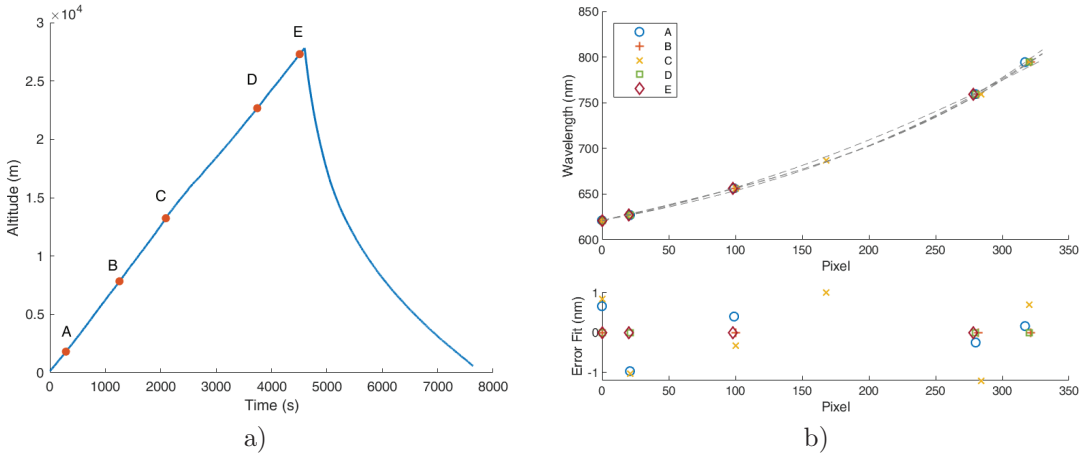

Figure 5. a) Five dots on the altitude profile identify the moment in which the signal A-E have been acquired. b) Calibration.

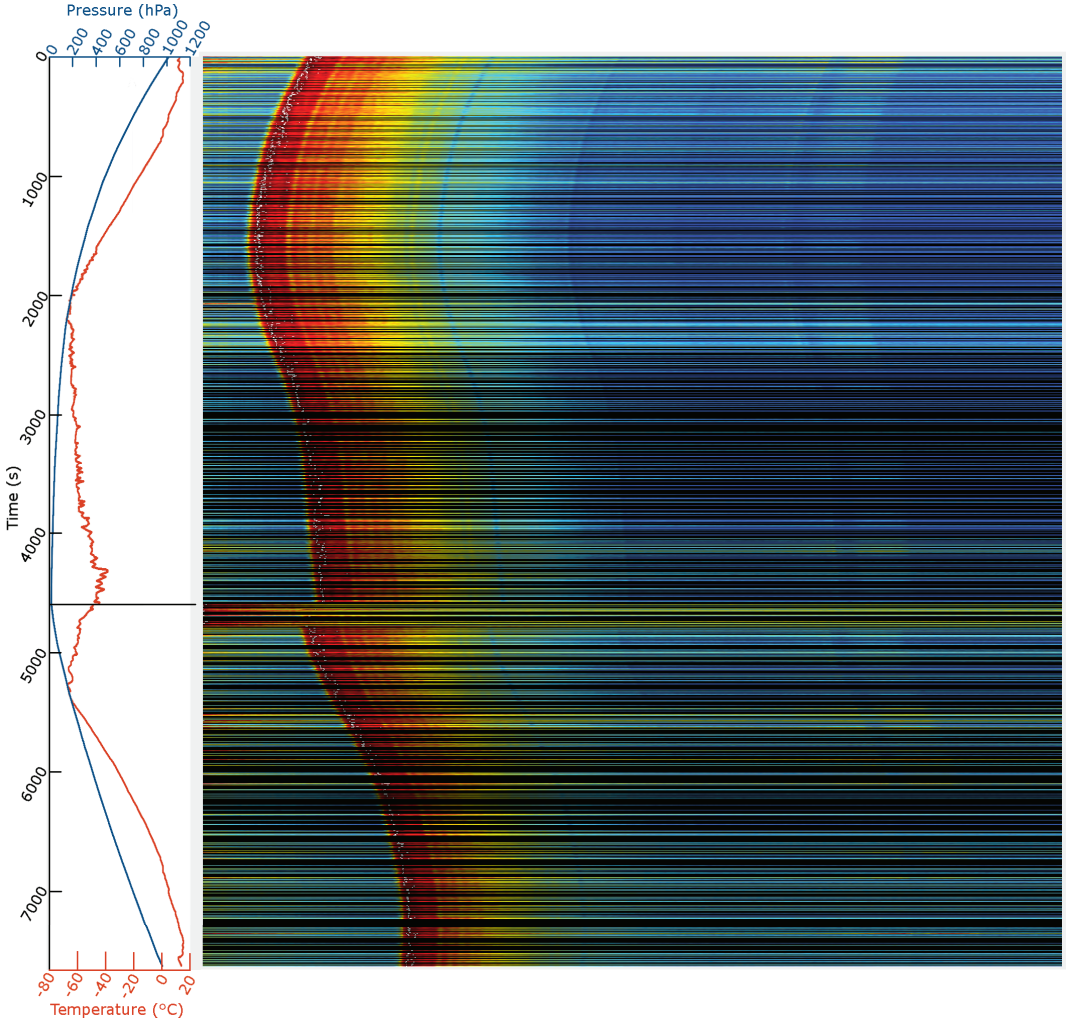

Figure 6. Spectra as a function of flight time with environmental conditions on the left panel.

5. CONCLUSIONS

In this work a static Fourier transform spectrometer has been tested with a flight on a sounding balloon. The flight campaign took place in October 2021 at the CNES "Centre d' Opérations Ballons" at Aire sur l'Adour, France. The results of these tests are showing that, for such an instrument, thermal drift issues appear to be still manageable as the actual limit to the instrument performance seems to be in the response to mechanical stresses and vibrations during flight. That information will lead us to the engineering of a new device addressing those issues.

ACKNOWLEDGMENTS

We desire to thank all the people from CNES that supported us during the flight campaign, in particular, and knowing we are mentioning just a few, André Vargas, Rubio Jean-Claude and Cruzel Serge.

Also, special thanks go to Pietro Fiorentini S. p. A. and its research and development staff (in particular Dr. Elena Meneghin) for granting access to their thermal test facility.

This work has been supported by ASI, Agenzia Spaziale Italiana, Agreement n. 2019-33- HH.0, for the payload realization and the flight opportunity has been provided by the European Commission in the frame of the INFRAIA grant 730790-HEMERA.

REFERENCES

[1] Jacquinot, P., "New developments in interference spectroscopy," *Reports on Progress in Physics* **23**, 267–312 (jan 1960).

[2] Harlander, J. M., *Spatial Heterodyne Spectroscopy: Interferometric Performance at any Wavelength Without Scanning.*, PhD thesis, University of Wisconsin, Madison (Feb. 1991).

[3] Roesler, F. L. and Harlander, J. M., "Spatial heterodyne spectroscopy: interferometric performance at any wavelength without scanning," in [*Optical Spectroscopic Instrumentation and Techniques for the 1990s: Applications in Astronomy, Chemistry, and Physics*], McNamara, B. J. and Lerner, J. M., eds., **1318**, 234 – 243, International Society for Optics and Photonics, SPIE (1990).

[4] Englert, C. R. and Harlander, J. M., "Flatfielding in spatial heterodyne spectroscopy," *Appl. Opt.* **45**, 4583–4590 (Jul 2006).

[5] Yi, Y., Zhang, S., Liu, F., Zhang, Y., and Yi, F., "Laboratory fabrication of monolithic interferometers for one and two-dimensional spatial heterodyne spectrometers," *Opt. Express* **25**, 29121–29134 (Nov 2017).

[6] Wu, X., Tan, Y., Yi, Y., Zhang, Y., and Yi, F., "Two-dimensional spatial heterodyne spectrometer for atmospheric nitrogen dioxide observations," *Opt. Express* **27**, 20942–20957 (Jul 2019).

[7] Kaufmann, M., Olschewski, F., Mantel, K., Solheim, B., Shepherd, G., Deiml, M., Liu, J., Song, R., Chen, Q., Wroblowski, O., Wei, D., Zhu, Y., Wagner, F., Loosen, F., Froehlich, D., Neubert, T., Rongen, H., Knieling, P., Toumpas, P., Shan, J., Tang, G., Koppmann, R., and Riese, M., "A highly miniaturized satellite payload based on a spatial heterodyne spectrometer for atmospheric temperature measurements in the mesosphere and lower thermosphere," *Atmospheric Measurement Techniques* **11**(7), 3861–3870 (2018).

[8] Frassetto, F., Cocola, L., Zuppella, P., Da Deppo, V., and Poletto, L., "High sensitivity static fourier transform spectrometer," *Opt. Express* **29**, 15906–15917 (May 2021).

[9] Frassetto, F., Cocola, L., Da Deppo, V., Poletto, L., and Zuppella, P., "High signal-to-noise ratio spectrometer based on static fourier transform interferometer (for hemera balloon flight)," in [*AIDAA XXV International Congress*], (2019).

[10] Frassetto, F., Cocola, L., Da Deppo, V., Poletto, L., and Zuppella, P., "Low noise fourier transform spectrometer for a balloon borne platform," in [*AIDAA XXVI International Congress*], (2021).